Archaeological Prospection
Archaeol. Prospect. **18**, 279–289 (2011)
Published online 20 September 2011 in Wiley Online Library
(wileyonlinelibrary.com) DOI: 10.1002/arp.421

A Generic Toolkit for the Visualization of Archaeological Features on Airborne LiDAR Elevation Data†

KEITH CHALLIS[1]*, PAOLO FORLIN[2] AND MARK KINCEY[1]

[1] *IBM Visual and Spatial Technology Centre, Birmingham Archaeology, University of Birmingham, Edgbaston, Birmingham, B15 2TT, UK*
[2] *Dipartimento di Filosofia, Storia e Beni Culturali, Università degli Studi di Trento, Piazza Venezia 41, 38122 Trento, Italy*

ABSTRACT A range of techniques have become established for the visualization and analysis of airborne LiDAR elevation data within the field of archaeology. In this paper we discuss the visualization of test data representing archaeological features in a variety of terrains using a suite of techniques, all available through generic geographical information system or image processing software. These comprise elevation shading using constrained colour ramps, slope analysis, hill-shading, principal component analysis of multi-azimuth hill-shading, local relief models and solar insolation modelling. The strengths and weaknesses of each technique are discussed and a generic toolkit, suited to the visualization of airborne LiDAR data for archaeological purposes, is presented. Copyright © 2011 John Wiley & Sons, Ltd.

Key words: LiDAR; archaeology; visualization; analytical techniques; toolkit

Introduction

Since its introduction to the archaeological community by Holden *et al*. (2002) the use of airborne LiDAR has become well established in archaeological research with applications ranging from landscape-scale geoarchaeological analysis (Carey *et al*., 2006; Howard *et al*., 2008), or the use of LiDAR survey to assist in compilation of systematic records of the historic environment (Challis *et al*., 2008) to applications utilizing some of the unique facets of LiDAR, for example its ability to penetrate the vegetation canopy to record underling archaeological features (Devereux *et al*., 2005; Doneus and Briese, 2006; Crow *et al*., 2007; Chase *et al*., 2011). Recent research has turned to new kinds of LiDAR sensor, for example the advantages offered over more usual discrete return data by full-waveform LiDAR (Doneus *et al*., 2008) and to relatively under-used aspects of LiDAR survey such as intensity data (Challis *et al*., 2011a, 2011b). As the use of LiDAR in archaeological research matures, a number of authors have considered data and image processing techniques that may be used to extract the maximum level of archaeological detail from LiDAR surveys to aid expert interpretation. Significant studies have either devised new analytical techniques, for example multivariate analysis of shaded relief images (Devereux *et al*., 2008) and modelling of local relief (Hesse, 2010) or cleverly adapted established methods of topographic analysis aimed at non-archaeological ends to provide new insights into landscape, for example the use of the sky-view factor outlined by Kokalj *et al.* (2011). However, it appears to the authors that much archaeological analysis of LiDAR data continues to rely on relatively unsophisticated visualization techniques, chiefly hill-shading from a single azimuth. This is compounded by the fact that the UK Environment Agency has supplied local authorities in England and Wales with LiDAR coverage visualized in this way as jpeg images, reinforcing amongst non-specialist users the

* Correspondence to: Keith Challis, IBM Visual and Spatial Technology Centre, Birmingham Archaeology, University of Birmingham, Edgbaston, Birmingham, B15 2TT, UK. E-mail: K.Challis@bham.ac.uk
†Correction added on 18 October 2011, after first online publication. Some additional acknowledgements have been added.

Received 24 June 2010
Accepted 5 August 2011

view that this is the preferred method of visualizing archaeological content in LiDAR surveys.

This paper attempts to address the trend to relatively unsophisticated visualization of LiDAR data. To achieve this we visualize test data in a variety of ways, using data representing a variety of terrain types and archaeological remains in order to compare the relative effectiveness of different techniques, make statements about their suitability in different scenarios, and present in conclusion suggestions for a generic toolkit of visualization techniques suitable for assisting in the archaeological analysis of LiDAR elevation data.

Methods

Test data

The study uses test data from four LiDAR surveys which combine a variety of terrain types and scales, differing archaeological content and a range of survey parameters from standard 2 m spatial resolution UK Environment Agency data to high resolution 0.5 m spatial resolution data. All data were collected using Optech discrete return LiDAR. The survey areas comprise (Figure 1):

(i) The Trent Valley, in Nottinghamshire, an alluviated valley floor with relatively little topographic variation and with well-defined low relief, earthworks, under pasture and examined using 2-m spatial resolution Environment Agency LiDAR.
(ii) The Dove Valley in Staffordshire, another alluviated valley floor with greater topographic variation than the Trent, and with extensive low-relief earthworks, principally related to past agricultural regimes (e.g. ridge and furrow) preserved under pasture and examined using 2-m spatial resolution Environment Agency LiDAR.
(iii) Pigwyn Roman Marching camp, Mynyd Myffai, Wales, upland moorland within the Brecon Beacons National Park, an area of high relief variation with subtle low-relief earthworks under mixed vegetation, examined using 1-m spatial resolution LiDAR collected by Infoterra Ltd.
(iv) Bentyfield Mine, Alston Moor, County Durham, upland moorland area of high relief, with substantial early industrial earthworks under mixed vegetation, examined using 0.5 m spatial resolution LiDAR collected by Infoterra Ltd.

Analytical and visualization techniques

Six analytical and visualization techniques were employed on the test data. The techniques were chosen to represent a range of published methods of analysis for discrete return airborne LiDAR and range from simple visualization to the generation of derived data products from the source digital surface model (DSM), which in turn require appropriate visualization. All techniques are accessible to users through the tools provided by a number of geographical information system (GIS) and image processing software (Table 1) and no bespoke scripting or programming was required to undertake the analysis reported here. Our work is undertaken exclusively using ESRI's ArcGIS 9.3, but could easily be duplicated in other software. Brief descriptions of the data and image processing methods adopted for each technique are provided below.

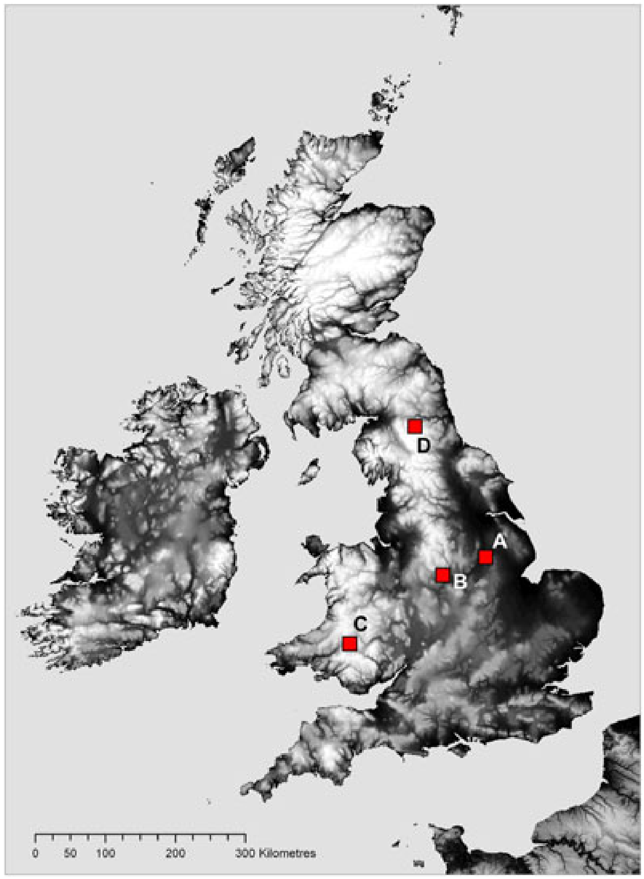

Figure 1. The British Isles showing the locations of the four test sites: (A) Trent Valley, (B) Dove Valley, (C) Pigwyn and (D) Bentyfield. This figure is available in colour online at wileyonlinelibrary.com/journal/arp.

Constrained colour shading uses analysis of the DSM to identify the range of elevation values within which topographic features of interest lie. Greyscale (or colour) shading is constrained to the elevation range of target features, maximizing the representation of detail within this limited range, but of necessity meaning that features

DOI: 10.1002/arp

Table 1. Geographical information system and image processing software offering LiDAR analysis functions.

Software	Operating system	Status	Colour shading	Slope analysis	Hill shading	PCA[a]	Terrain filtering	Solar insolation
ArcGIS 9/10	Windows	Commercial	X	x	x	x	x	x
ArcView 3.1	Windows	Commercial	X	x	x		x	x
Envi	Windows	Commercial	X	x	x	x	x	x
Grass	Windows/Linux/Mac	Open Source	X	x	x	x	x	x
Idrisi	Windows	Educational	X	x	x	x	x	
Imagine	Windows	Commercial	X	x	x	x	x	x
MapInfo	Windows	Commercial	X	x	x			
QGis	Windows/Linux/Mac	Open Source	X	x	x			
Saga GIS	Windows/Linux	Open Source	X	x	x		x	x

[a]Principal component analysis.

outside of this range are not represented. The technique has been particularly used in areas of low relief variation (for example valley floors) to illustrate geomorphological features (e.g. Challis, 2006).

Generic GIS **slope analysis** calculates the slope of each cell within a raster DSM by determining the maximum rate of elevation change between each cell and its neighbours. Slope calculations, either as a percentage slope or a degree slope are stored in a new raster array and visualized as a greyscale image with grey values representing slope.

Hill-shading algorithms calculate the shading for each cell in a DSM by determining illumination values from a hypothetical light source. The great advantage of hill-shading is that the resulting visualization looks very much like a natural landscape with uniform surface cover and illuminated by low sunlight; as such it is both visually pleasing and easy for non-technical users to interpret. The angle of inclination and azimuth of the hypothetical light source may be varied to achieve differing illumination effects, and in particular to overcome the chief flaw of this technique, its failure to illuminate topographic features parallel to the azimuth of the illumination source. In spite of its shortcomings, hill-shading represents the single most used visualization technique for archaeological LiDAR data, although a number of authors have commented on its limitations and proposed routines to at least partially overcome these (e.g. Crutchley (2006), who advocates shading each scene from at least four azimuths). Devereux *et al.* (2008) developed a sophisticated variation of hill-shading by adopting the multivariate statistical technique of **principal component analysis** (PCA) to examine the product of a sequence of hill-shaded images of the same scene with systematic variation in the azimuth of the illumination source. Component images present new, summary views of the data with redundancy removed. In the present study we have followed Deveraux *et al.*'s method by generating 16 hill-shaded images of our source data, each with a 22.5° variation in azimuth, as the source for principal component analysis. Results may be visualized as a greyscale (for single components) or as a false colour multiband image, allowing three components to be viewed together.

Local-relief models (LRMs) attempt to mitigate the masking affect of natural topographic variation on archaeological earthworks by subtracting a generalized digital terrain model, generated by a low-pass filter, from the original DSM. The effect is to produce a new representation of relief containing only the archaeological earthworks. The method developed by Hesse (2010) is adopted here as it adds an additional, refining, stage to the generation of the local relief model. Low-relief models are generally visualized using a graded binary colour scale, where one colour represents maximum negative values and the other maximum positive.

Solar insolation models (SIMs) quantify the amount of the Sun's energy received at the Earth's surface. The models require complex calculations, but GIS provide a means to rapidly calculate area solar isolation using digital terrain models (Dubayah and Rich, 1995). In brief, SIMs involve the calculation of an upward-looking hemispherical viewshed, based on surrounding topography, for each location on the DSM. Solar insolation is modelled by overlaying the hemispherical viewshed on direct and diffuse sunmaps, to allow calculation of direct, diffuse and global solar radiation and the duration of radiation. The Sky-View factor modelled by Kokalj *et al.* (2011) is based on calculation of the area of visible sky for each location within the terrain model, that is the area of unobscured sky is seen in each hemispherical viewshed. We prefer to use calculations of solar insolation as these offer four solutions for each DSM, which provides more visualization choices, additionally variations in solar insolation may be used to help determine areas of landscape particularly suited to past activity based on the amount of sun received.

DOI: 10.1002/arp

Figure 2 shows graphically the variations in direct, diffuse and global solar radiation received at ten test locations over the course of a year. Results clearly show that significantly less sunlight is received at locations within negative archaeological features and highlights the principle underlying this technique. Since the variation in insolation due to earthworks is in addition to that due to base topography, and as SIMs usually summarize received radiation over a period of time (a day, a month, etc.), the shadow effects resulting from the single illumination azimuth used in hill-shade calculations are largely removed. In this study we have generally used calculations of sum monthly solar insolation. Total insolation varies considerably by month throughout the year (Figure 2) and we have found that data for late spring (usually May–June) provide the best visualization opportunities. In all cases data are visualized as a simple greyscale with grey values representing sum total insolation.

Results

Results from the full suite of techniques are shown in Figures 3–6 and discussed below. With the exception of the elevation and local relief visualizations (which require case-specific values) a standard deviation stretch has been used to enhance the contrast of each graphic to aid clarity of presentation.

Low-relief landscapes

Effective visualization of archaeological earthworks in low-relief landscapes is relatively straightforward as

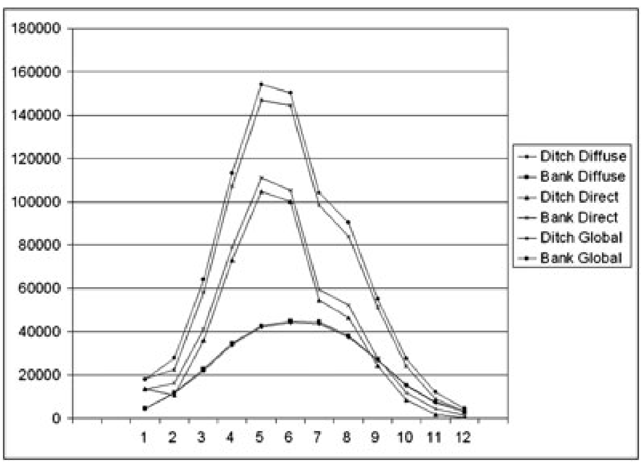

Figure 2. Line graph showing the variations in the total diffuse, direct and global solar radiation per month received at test locations on the top of an earthwork archaeological bank and at the bottom of an adjacent ditch for each month over a calendar year.

the masking effects of significant changes in base elevation are largely absent; the issue becomes one of uniformly highlighting features of varying scale and orientation.

In many cases, use of constrained colour shading can be effective, for example in identifying the earthworks of a post-medieval fort shown in Figure 3, and has the advantage of presenting information on the scale of earthwork features, allowing rapid assessment of, for example, depth of ditches. However, even slight variations in base elevation render this technique less useful; for example the earthwork ridge and furrow in Figure 4 are largely obscured by variation in base topography.

Visualization of slope severity is, predictably, effective for earthworks with steeply sloping sides (Figure 3) and provides useful insight into the character of the earthworks, but is markedly less successful in identifying the gently sloping earthworks of ridge and furrow (Figure 4).

Hill-shaded visualization is quite effective for earthwork features with well-defined edges, where the detrimental impact of single azimuth shading is largely overcome (Figure 3) and the character of the earthworks effectively represented. However, in the case of earthworks with varied alignment, such as the several furlongs of ridge and furrow seen in Figure 4, hill-shading fails to adequately highlight subtle features as well as those aligned close to the azimuth of the illumination source. Principal component analysis of multiple azimuth illumination enhances visibility of subtle features and overcomes some of the azimuth-related difficulties (Figure 3 and 4). In general false colour composite images of statistically significant components reveal most, but are more challenging to interpret than single components; in transcribing archaeological detail it is most effective to view single components (usually 1–3) in sequence.

Models of solar insolation are particularly effective at visualizing earthwork features. We compare the effectiveness of direct, diffuse and global solar radiation models and duration of radiation in Figures 3 and 4. Direct solar radiation is to some extent affected by azimuth, since it models illumination from the exact sky path of the Sun. There are advantages to this fact, since modelling insolation for occasions when the Sun is low in the sky may produce striking shadow effects; however, the technique is open to many of the same azimuth-related problems as conventional hill-shading. In contrast, diffuse solar radiation is usually based on a uniform sky model in which the azimuth-related aspects of illumination are suppressed. Insolation is therefore directly related to each location's hemispherical viewshed,

DOI: 10.1002/arp

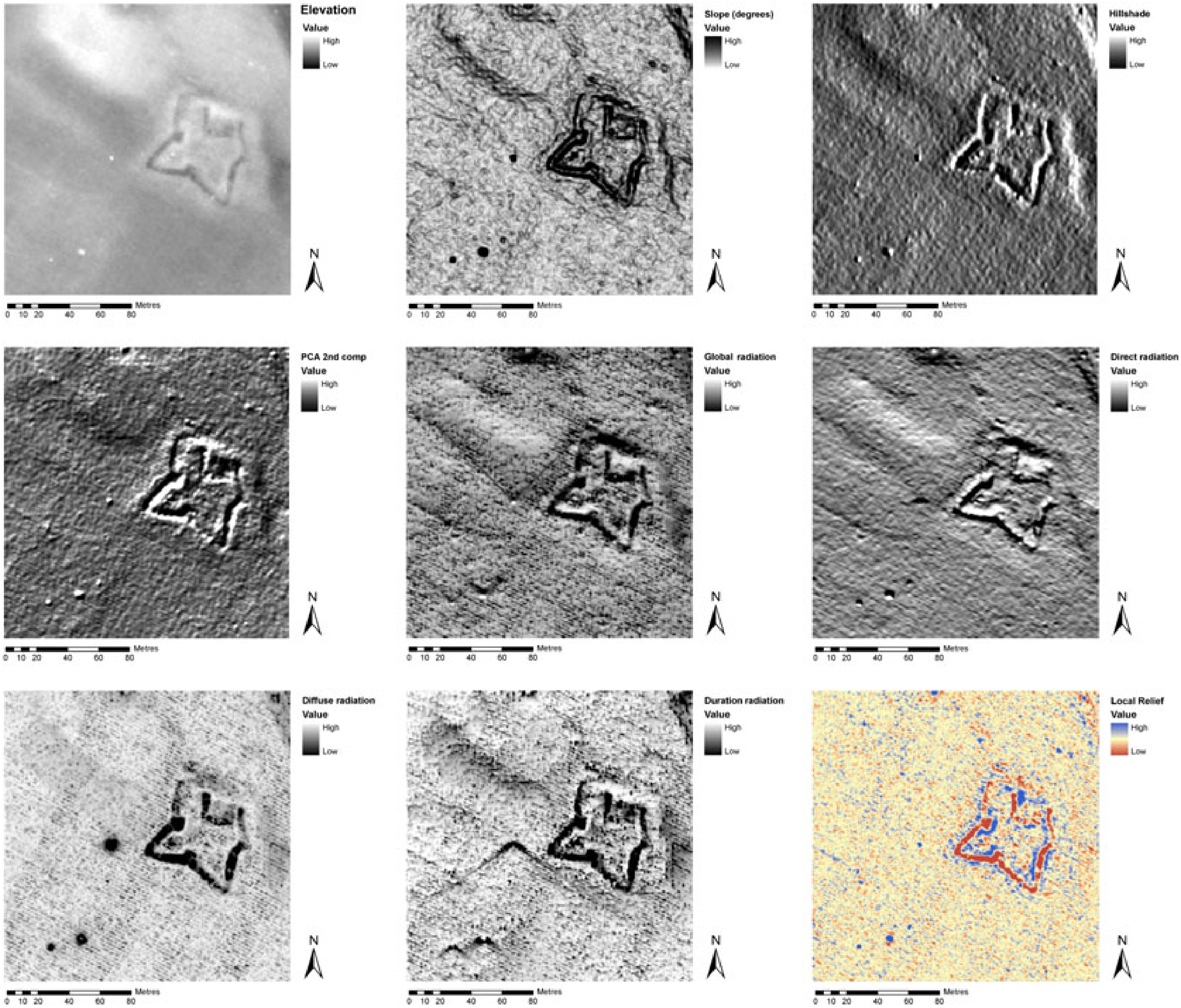

Figure 3. Earthworks of an English Civil War star fort at Crankley Point, Newark on Trent, Nottinghamshire as evidenced by 2-m spatial resolution Environment Agency LiDAR data using the various visualization and analysis methods discussed, from top left: elevation, slope severity, hill-shade, 2nd component of PCA of hill-shade, global SIM, direct SIM, diffuse SIM, direct duration SIM and local relief. This figure is available in colour online at wileyonlinelibrary.com/journal/arp.

although areas of deep shadow resulting from significant topographic depressions may lack definition of detail. We have found this visualization technique almost universally effective in highlighting archaeological earthworks of varying magnitude and form and on any alignment.

Global solar radiation, the total amount of the Sun's energy received at each location and a product of the direct and diffuse components, produces visualizations with less marked azimuth effects and a greater sense of the form of earthworks than is usually apparent in models of diffuse insolation. Models of the duration of solar radiation (i.e. the amount of direct solar radiation in hours per time period given a clear sky), although highlighting topographically induced variations, including those due to earthworks, tend to suppress archaeological detail and are not generally an improvement on other methods of analysis.

We have found local relief models to be of some use in visualizing and isolating well-defined archaeological earthworks in low-relief landscapes (Figure 3). The technique clearly identifies positive and negative features and the scale of the earthworks is immediately apparent, however, subtleties in the form of earthworks are largely lost as features are shown either as positive or

DOI: 10.1002/arp

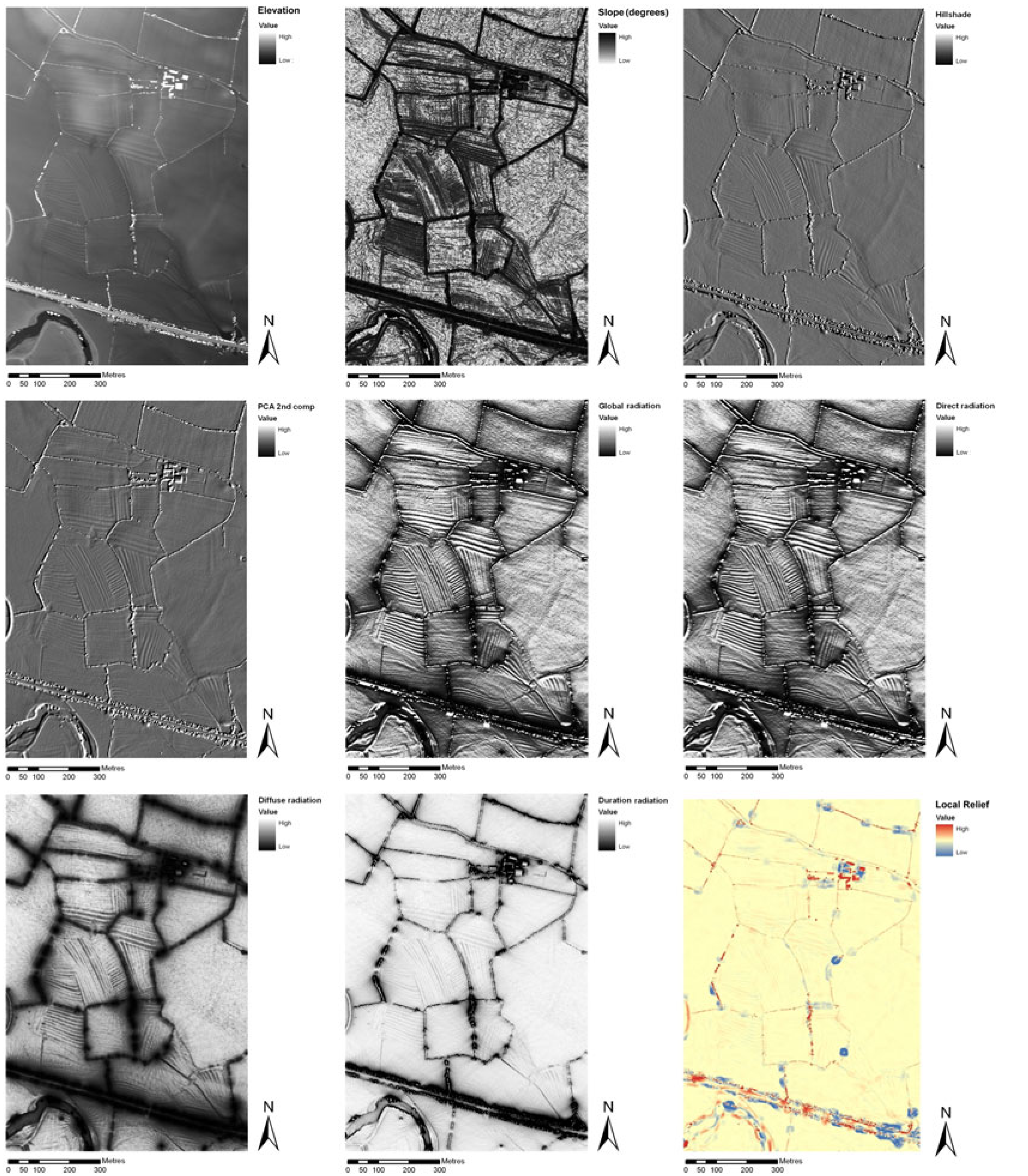

Figure 4. Earthworks of several adjacent furlongs of ridge and furrow in the Dove Valley, Staffordshire as evidenced by 2-m spatial resolution Environment Agency LiDAR data, from top left: elevation, slope severity, hill-shade, 2nd component of PCA of hill-shade, global SIM, direct SIM, diffuse SIM, direct duration SIM and local relief. This figure is available in colour online at wileyonlinelibrary.com/journal/arp.

DOI: 10.1002/arp

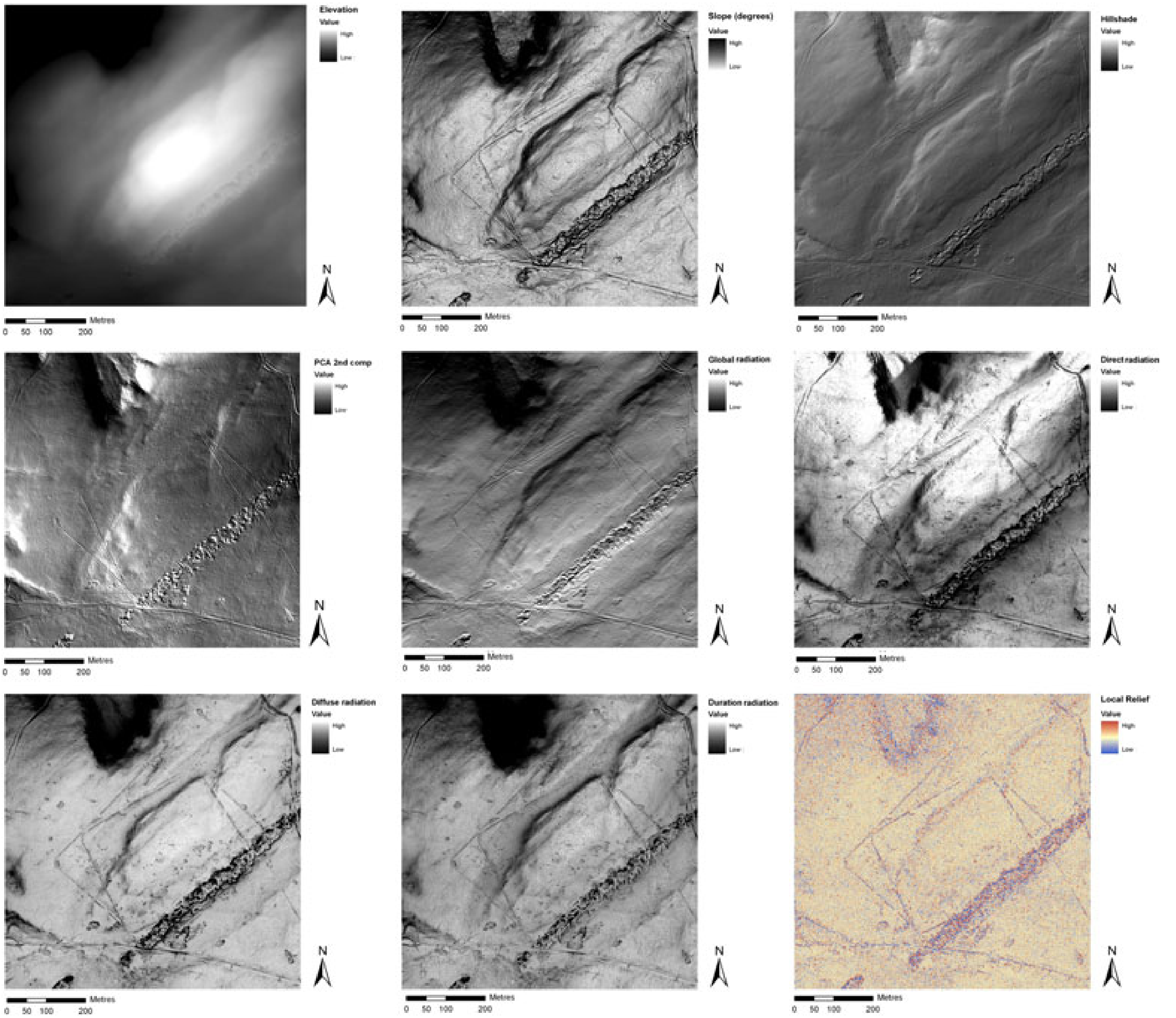

Figure 5. Earthworks of two superimposed Roman marching camps at Y Pigwyn, near Brecon, Wales as evidenced by 1 m spatial resolution LiDAR, from top left: elevation, slope severity, hill-shade, 2nd component of PCA of hill-shade, global SIM, direct SIM, diffuse SIM, direct duration SIM and local relief. This figure is available in colour online at wileyonlinelibrary.com/journal/arp.

negative. In areas of subtle earthworks (such as the ridge and furrow in Figure 4) the technique is less effective as high-magnitude features tend to mask the visibility of lower magnitude earthworks. This limitation can to some extent be overcome with a carefully selected colour ramp at the point of final visualization, but in many cases the results do not significantly improve on that achievable with the unprocessed DSM.

High-relief landscapes

In areas of high natural relief, elevation-based shading is of little use as variation in the background relief overwhelms any variation caused by target features, rendering them invisible.

Visualization of slope severity is, however, particularly effective at highlighting even slight earthworks, so long as they are defined by features with reasonably steeply sloping slides, so at both Pigwyn (Figure 5) and Bentyfield (Figure 6) the majority of archaeological earthworks are represented in the slope severity images due to their steep, well defined edges.

As might be expected hill-shaded visualization are of limited usefulness. At Pigwyn the majority of the south side of the two superimposed Roman marching camps are not apparent on hill-shaded images illuminated from the default 315° azimuth (Figure 5). The

DOI: 10.1002/arp

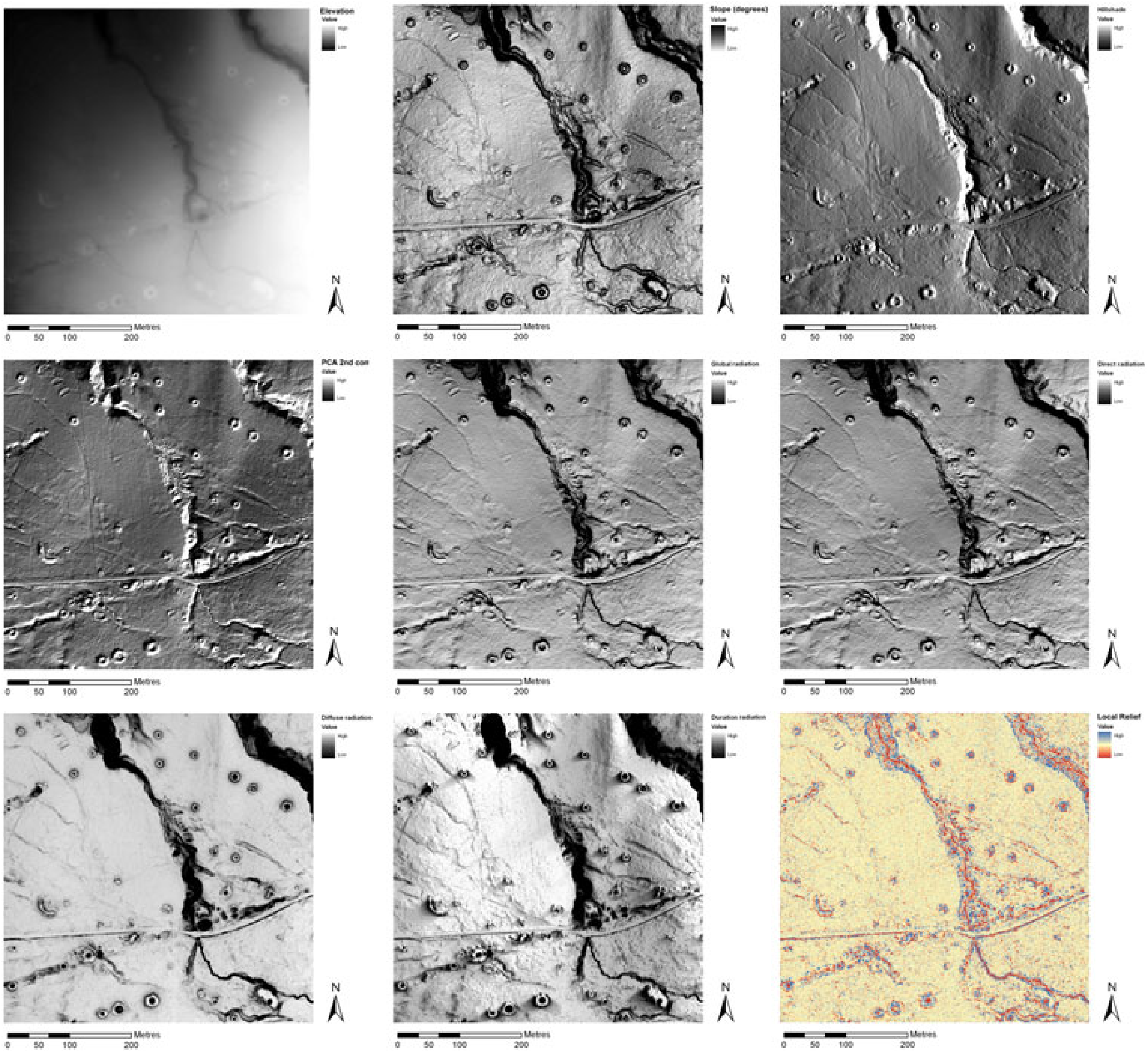

Figure 6. Earthworks of post-medieval mining remains at Bentyfield, Alston Moor, County Durham, as evidenced by 0.5-m spatial resolution LiDAR, from top left: elevation, slope severity, hill-shade, 2nd component of PCA of hill-shade, global SIM, direct SIM, diffuse SIM, direct duration SIM and local relief. This figure is available in colour online at wileyonlinelibrary.com/journal/arp.

situation is somewhat better at Bentyfield where well-defined industrial features on an upland plateau are quite clearly visualized (Figure 6). Principal component analysis of multi-azimuth shading improves little on the visualization of features at Pigwyn, where individual components succeed in highlighting only parts of the entire array of earthworks (Figure 5).

The impact of solar insolation modelling on enhancing earthwork visibility is most marked at Pigwyn, where all insolation models improve on conventional hill shading. Models of diffuse solar radiation (Figure 5) and duration of direct radiation (Figure 6) succeed in visualizing earthworks, as neither are affected by the azimuth of illumination. The earthworks of the Roman marching camps are laid bare with startling clarity by these techniques. However, areas of deep natural gullying are too heavily shaded for detail to be apparent, and the steep gullying of post-medieval mining (here magnified by data artefacts generated by vegetation removal algorithms) create a linear scar across the Roman camps, which is poorly rendered with insolation models and is better understood in the slope severity model. Clearly this indicates that in many circumstances consideration of recent landscape history and underlying materials will influence the choice of appropriate visualization and analytical techniques.

DOI: 10.1002/arp

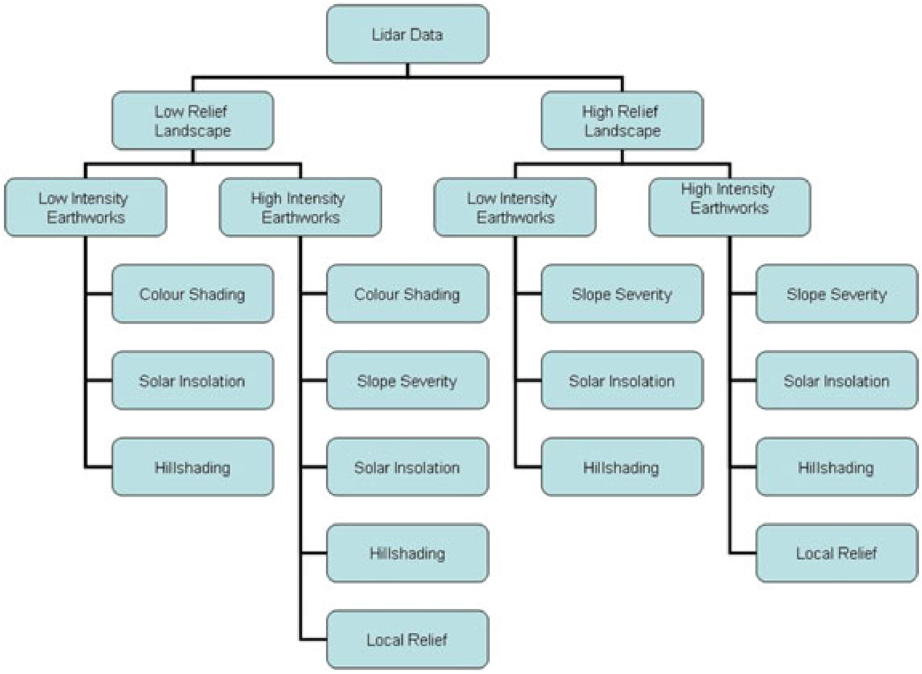

Figure 7. A proposed analytical workflow for LiDAR data in areas of low relief and high relief with differing earthwork types using the toolkit approach outlined in the text. This figure is available in colour online at wileyonlinelibrary.com/journal/arp.

At both Pigwn and Bentyfield local relief modelling is able to highlight the majority of archaeological earthworks, including those subtle earthworks invisible using hill-shading techniques (Figures 5 and 6). However, the overall picture is less clear than that achieved through slope or insolation modelling. Although useful information on the scale of the earthworks is immediately apparent, recourse to other visualization methods that better reveal earthwork form is necessary for a full interpretation.

A toolkit for LiDAR analysis

It is clear that a number of techniques are of use for visualizing archaeological evidence on airborne LiDAR data and that these succeed or fail largely as a result of the scale and form of the target features. It is important to recognize that it is likely that in any landscape no single technique will reveal all archaeological detail, and that well-judged use of a suite of techniques coupled with careful and well-informed interpretation will serve to reveal both the presence and the morphological form of earthwork features recorded by airborne LiDAR. Below, we present our suggestions for a toolkit for archaeological LiDAR analysis, summarized in Figure 7.

(i) In all scenarios we suggest that the sole use of conventional hill-shading from a single azimuth should be avoided. We suggest that this technique is used only when appropriate, chiefly to visualize discrete, well-defined earthworks. We have found that PCA shading provides little additional benefit for the computational overhead.
(ii) In areas of low natural relief variation (river valleys, plateau) elevation shading will provide acceptable results and is to be preferred to hill-shading as it is unaffected by the orientation of target features.
(iii) In most circumstances, well defined archaeological features, *whatever their orientation*, will be most clearly visible on models of slope severity. We suggest that this, rather that hill-shading, is a more appropriate general visualization method for most circumstances.
(iv) Solar insolation models for diffuse and global solar radiation provide the best overall visibility of archaeological earthworks of any scale and are virtually unaffected by target feature orientation, although some features, particularly those of low magnitude, may be poorly visualized where located on deep natural depressions that remain largely in shade.
(v) Where well defined earthworks are identified by other techniques local relief models provide visual information on the scale of earthwork features that is not otherwise readily apparent.

A range of other analysis and visualization methods exist and are suited, to a greater or lesser degree, to use

DOI: 10.1002/arp

with LiDAR data. In particular high-pass filtering (this emphasizes high frequency change, such as earthworks, at the expense of background topography), and DSM derived products such as indices of slope curvature, may have a place in regular LiDAR analysis and visualization for archaeological purposes.

The tools necessary to undertake all of the analysis steps discussed here are available in modern GIS and image processing software via simple menu driven interfaces, which require no expert knowledge to use, but demand some understanding of the meaning of results to interpret. In addition, free Open Source GIS such as SAGA, Quantum GIS and GRASS provide access to many of the tools required (Table 1). We suggest that to gain the maximum benefit from LiDAR data archaeologists should avoid reliance on a single visualization technique, but rather work with a suite of complementary techniques, recognizing that some are more suited to feature detection and others to the elaboration of the form of features once detected. Such a toolkit-based workflow represents a mature response to the richness of LiDAR data and, given initial learning time, is likely to significantly increase the speed and accuracy of archaeological LiDAR interpretation in the longer term.

Conclusions

It is our conclusion that the most frequently used visualization technique for archaeological LiDAR analysis, hill-shading, is in fact the least useful for visualizing archaeological detail in the majority of circumstances. Reliance on hill-shading from a single azimuth is likely to significantly underrepresent the amount of archaeological information present in typical LiDAR data and this *caveat* should be borne in mind, in particular when examining static images visualized with single azimuth shading, as for example provided by Environment Agency. We suggest that reliance on such imagery should be treated with extreme caution and that wherever possible specifications for the archaeological analysis of LiDAR data should include provision for multimethod visualization using the toolkit-based approach we have outlined.

Acknowledgements

The authors would like to thank the Dipartimento di Filosofia, Storia e Beni Culturali, Università degli Studi di Trento and the College of Arts and Law, University of Birmingham for supporting Paolo Forlin in his visiting fellowship with the Vista Centre. PF thanks Elisa Possenti (teaching fellow of Medieval Archaeology, Department of Philosophy, History and Cultural Heritage, University of Trento) and Gian Pietro Brogiolo (Professor of Medieval Archaeology and scientific director of APSAT project, Department of Archaeology, University of Padua) for their supervision of his research. KC and MK acknowledge a great debt of gratitude to Dr Ziga Kokalj for introducing us to sky-view factor and so providing the kernel of an idea for the research reported here. The authors acknowledge the help of English Heritage and in particular Stewart Ainsworth for the supply of lidar data used in Figure 6.

References

Carey C, Brown T, Challis K, Howard AJ, Cooper L. 2006. Predictive modelling of multiperiod geoarchaeological resources at a river confluence: a case study from the Trent–Soar, UK. *Archaeological Prospection* **13**(4): 241–250.

Challis K. 2006. Airborne laser altimetry in alluviated landscapes. *Archaeological Prospection* **13**(2): 103–127.

Challis K, Kokalj Z, Kincey M, Moscrop D, Howard AJ. 2008. Airborne lidar and historic environment records. *Antiquity* **82**(318): 1055–1064.

Challis K, Carey C, Kincey M, Howard AJ. 2011a. Assessing the preservation potential of temperate lowland alluvial sediments using airborne lidar intensity. *Journal of Archaeological Science* **38**: 301–313.

Challis K, Carey C, Kincey M, Howard AJ. 2011b. Airborne Lidar Intensity And Geoarchaeological Prospection In River Valley Floors. *Archaeological Prospection* **18**: 1–13.

Chase AF, Chase D, Weishampel J, *et al.* 2011. Airborne LiDAR, archaeology, and the ancient Maya landscape at Caracol, Belize. *Journal of Archaeological Science* **38**: 387–398.

Crow P, Benham S, Devereux BJ, Amable GS. 2007. Woodland vegetation and its implications for archaeological survey using Lidar. *Forestry* **80**(3): 241–252.

Crutchley S. 2006. Light detection and ranging (lidar) in the Witham Valley, Lincolnshire: an assessment of new remote sensing techniques. *Archaeological Prospection* **13**(4): 251–257.

Devereux BJ, Amable GS, Crow P, Cliff AD. 2005. The potential of airborne lidar for detection of archaeological features under woodland canopies. *Antiquity* **79**(305): 648–660.

Devereux BJ, Amable GS, Crow P. 2008. Visualisation of LiDAR terrain models for archaeological feature detection. *Antiquity* **8**(316): 470–479.

Doneus M, Briese C. 2006. Digital terrain modelling for archaeological interpretation within forested areas using full-waveform laser scanning. *Proceedings of the 7th International Symposium on Virtual Reality, Archaeology and Cultural Heritage* (VAST 2006): 155–162.

Doneus M, Briese C, Fera M, Janner M. 2008. Archaeological prospection of forested areas using full-waveform airborne laser scanning. *Journal of Archaeological Science* **35**(4): 882–893.

Dubayah R, Rich PM. 1995. Topographic solar radiation models in GIS. *International Journal of Geographical Information Science* **9**(4): 405–419.

DOI: 10.1002/arp

Hesse R. 2010. LiDAR-derived local relief models (LRM) – a new tool for archaeological prospection. *Archaeological Prospection* **17**(2): 67–72.

Holden N, Horne P, Bewley RH. 2002. High-resolution digital airborne mapping and archaeology. In Aerial Archaeology: Developing Future Practice, Bewley R, Raczkowski W (eds). NATO Series 1, Vol. **337**, IOS Press: Amsterdam; 173–180.

Howard AJ, Brown AG, Carey CJ, Challis K, Cooper LP, Kincey M, Toms P,. 2008. Archaeological Resource Modelling in Temperate River Valleys: A Case Study from the Trent Valley, UK. *Antiquity* **82**: 1040–1054.

Kokalj Ž, Zakšek K, Oštir K. 2011. Application of the sky-view factor for the visualization of historic landscape features in lidar derived relief models. *Antiquity* **85** (327): 263–273.